IEEE Access
Multidisciplinary | Rapid Review | Open Access Journal

Received 18 May 2023, accepted 21 June 2023, date of publication 27 June 2023, date of current version 5 July 2023.

Digital Object Identifier 10.1109/ACCESS.2023.3289821

RESEARCH ARTICLE

Optimal Capacity and Cost Analysis of Hybrid Energy Storage System in Standalone DC Microgrid

TERAPONG BOONRAKSA[1], WATCHARAKORN PINTHURAT[2], PINIT WONGDET[3], PROMPHAK BOONRAKSA[4], BOONRUANG MARUNGSRI[3], (Member, IEEE), AND BRANISLAV HREDZAK[5], (Senior Member, IEEE)

[1]School of Electrical Engineering, Rajamangala University of Technology Rattanakosin, Nakhon Pathom 73170, Thailand
[2]Department of Electrical Engineering, Rajamangala University of Technology Tawan-ok, Chanthaburi 22210, Thailand
[3]School of Electrical Engineering, Suranaree University of Technology, Nakhon Ratchasima 30000, Thailand
[4]School of Electrical Engineering, Rajamangala University of Technology Suvarnabhumi, Nonthaburi 11000, Thailand
[5]School of Electrical Engineering and Telecommunications, University of New South Wales, Sydney, NSW 2052, Australia

Corresponding author: Boonruang Marungsri (bmshvee@sut.ac.th)

This work was supported in part by the Rajamangala University of Technology Rattanakosin; in part by the Rajamangala University of Technology Tawan-ok; in part by the Rajamangala University of Technology Suvarnabhum; and in part by the Suranaree University of Technology, Thailand.

ABSTRACT DC microgrid systems have been increasingly employed in recent years to address the need for reducing fossil fuel use in electricity generation. Distributed generations (DGs), primarily DC sources, play a crucial role in efficient microgrid energy management. Energy storage systems (ESSs), though vital for enhancing microgrid stability and reliability, currently lack cost-effectiveness. Each ESS technology serves a specific purpose, suggesting that hybridizing these technologies can improve microgrid stability and reliability while extending the ESS's lifespan. This paper proposes an optimization of the capacity and cost of a hybrid ESS, comprising a battery and a supercapacitor, in a standalone DC microgrid. This optimization is achieved by calculating the cut-off frequency of a low-pass filter (LPF). The supercapacitor supplies the high fluctuation component of renewable power generation and load demand, while the battery caters to the low fluctuation component. To minimize the designed objective function, including the total net present value (NPV) and replacement cost of the hybrid ESS, a meta-heuristic strategy called the Whale optimization algorithm (WOA) is employed within a MATLAB environment. The optimization takes into account real PV power, wind turbine power and load demand. The results show that reducing power fluctuation for the battery can lower the cost of the hybrid ESS. Compared to a battery-only microgrid system with an NPV_{total} of \$6,153,059, the hybrid ESS has an NPV_{total} of \$5,413,846. Thus, the hybrid ESS can reduce the total cost of the entire project by 12.01% compared to the system with only a battery. Consequently, the hybrid ESS's total system life-cycle cost is lower than that of a system using only a battery.

INDEX TERMS Battery energy storage system, hybrid energy storage system, low-pass filter, battery, supercapacitor, whale optimization algorithm.

NOMENCLATURE

β	Rate of self-discharge of battery.
Δt	Circle time.
η_{b_ch}	Charge efficiency of battery.
η_{b_dis}	Discharging efficiency of battery.
η_{sc_ch}	Charge efficiency of supercapacitor.
η_{sc_dis}	Discharging efficiency of supercapacitor.
$\vec{a}$	Convergence factor.
$\vec{A}$, $\vec{C}$, $\vec{D}$	Coefficient vectors.
$\vec{D}^*$	Distance between the i-th whale and the current optimal position.

The associate editor coordinating the review of this manuscript and approving it for publication was Behnam Mohammadi-Ivatloo.

$\overrightarrow{X}$	Current position vector.
$\overrightarrow{X}_{gbest}$	Position vector of the best solution.
$\overrightarrow{X}_{r}$	Random position vector.
σ	Rate of self-discharge of supercapacitor.
b	Constant coefficient used to define the spiral pattern.
C_{b_E}	Cost per energy of battery.
$C_{b\_install}$	Initial installation cost of battery.
$C_{b\_o\&m}$	Operation and maintenance cost of battery.
C_{b_P}	Cost per power of battery.
$C_{install}$	Initial installation cost of hybrid ESS.
C_{sc_E}	Cost per energy of supercapacitor.
$C_{sc\_install}$	Initial installation cost of supercapacitor.
$C_{sc\_o\&m}$	Operation and maintenance cost of supercapacitor.
C_{sc_P}	Cost per power of supercapacitor.
d	Discount rate.
E_{b_based}	Usable energy capacity of battery.
E_{b_rated}	Rated energy capacity of battery.
E_b	Battery energy capacity.
E_{sc_based}	Usable energy capacity of supercapacitor.
E_{sc_rated}	Rated supercapacitor energy capacity.
E_{sc}	Supercapacitor energy capacity.
f_c	Cut-off frequency of low-pass filter.
l	Random number between [0,1].
L_b	Cycle life of battery.
L_P	Cycle life of project.
L_{sc}	Cycle life of supercapacitor.
N_{b_re}	Number of battery replacement.
N_{sc_re}	Number of supercapacitor replacement.
$NPV_{b\_o\&m}$	Net present value of battery operation and maintenance cost.
$NPV_{b\_replace}$	Net present value of battery replacement.
$NPV_{o\&m}$	Net present value of the operation and maintenance cost throughout the project.
$NPV_{replace}$	Net present value of hybrid ESS replacement.
$NPV_{sc\_o\&m}$	Net present value of supercapacitor operation and maintenance cost.
$NPV_{sc\_replace}$	Net present value of supercapacitor replacement.
NPV_{total}	Net present value of total cost of hybrid ESS.
P_{b_ch}	Battery charged active power.
P_{b_dis}	Battery discharged active power.
P_{b_rated}	Rated battery active power.
P_{b_ref}	Active power reference of battery.
P_{H_ref}	Reference active power of hybrid ESS.
P_{Load}	Active power of load demand.
P_{PV}	Active power of PV system.
P_{sc_ch}	Supercapacitor charged active power.
P_{sc_dis}	Supercapacitor discharged active power.
P_{sc_rated}	Rated supercapacitor active power.
P_{sc_ref}	Active power reference of supercapacitor.
P_{WT}	Active power of WT system.
r_{rand}	Random vector in [0,1].
SoC_b	Battery state of charge.
SoC_{sc}	Supercapacitor state of charge.
T	Maximum iteration.
t	Current iteration.
T_f	Time constant of low-pass filter.
T_s	Sampling interval value.

I. INTRODUCTION

At present time, microgrid systems, in which the DGs are heavily integrated into the power grids, are gaining more attention from researchers and system operators. In Thailand, the most widely used DGs are solar PV and wind turbine (WT) power generations [1]. Grid-connected renewable energy resources (RESs) are viable solutions to meet rapidly growing demands in microgrid systems. However, the intermittent and volatile nature of the RESs hinders their performance and prevents them from being used efficiently. It is a common practise to combine the RESs with an efficient battery energy storage system (BESS). Lead-acid batteries play an important role in stationary ESS. Recently, lithium-ion battery (Li-ion) technology has been developed, and its price has continued to decrease [2]. A technological and economic analysis of the Li-ion and lead-acid batteries integrated into grid-connected power networks and PV systems was conducted by considering commercial load profiles [3]. The performance of the mentioned battery technologies is also greatly affected by the rate of charge and discharge, which in turn gradually decreases their capacity. Thus, the employed battery required optimal sizing of the entire system to maximize its efficient utilization. Therefore, both types of batteries are viable options in the microgrid system [3], [4].

At present, ESSs come in many forms, sizes and features. The most widely used ESS in the microgrid system is the battery because it can store a large amount of energy. Also, the battery has a fast response time, is easy to control, and has many types and sizes available on the market. A battery can support charging and discharging with constant characteristics according to electrochemical and chemical reactions. Therefore, the constant charging and discharging characteristics of current can extend the battery's lifetime. However, electricity generation from the RESs and load demands in power systems are characterized by inconsistency due to rapid increases or decreases, resulting in high fluctuations in the current charging or discharging of the battery. Therefore, other technologies of the ESSs are necessary for enhancement of system efficiency [5], [6], [7]. Hybrid ESS combines the advantages of different ES technologies. The common use of hybrid ESSs is between batteries and supercapacitors, in which the supercapacitor is suitable due toÂ its ability to respond to charge and discharge many times faster than batteries. However, the supercapacitor has a small energy capacity and is suitable for supplying or receiving power in the form of surges in a short time with less heat than a battery because of its low internal resistance [8]. Using hybrid ESS

between battery and supercapacitor can increase power system stability and reliability and prolong the battery's lifetime.

A microgrid system is a key component in extending modern electricity services to power consumers. A detailed cost analysis of battery in a microgrid can provide the high performance of a Li-ion or lead-acid battery and minimize total cost [9]. The analysis and application of hybrid ESSs in small standalone DC microgrids for remote areas have attracted widespread attention [10]. The volatile nature of wind energy produces large fluctuations in power generation, which in turn can have serious consequences for the battery's lifetime [11]. The uncertainty of the RESs has inspired researchers to combine different technologies for the energy sources, including energy storage devices, to ensure the reliability of the microgrid. Intelligent energy management systems (EMS) are used to define the energy flow between hybrid renewable energy systems, energy storage, and the power grid [12]. High-capacity lithium-ion battery and high-power supercapacitor are the ideal ESS for a DC microgrid. It is important to have a power management strategy that increases bus voltage feedback compensation and can keep the bus voltage within a reasonable range due to load fluctuations [13]. Energy exchanged between energy storage devices (ESDs) by utilizing a low-pass filter (LPF) can reduce the size of the ESS without negatively impacting the battery lifetime [14], [15]. The operating cost of a battery is determined by the depth of discharge (DOD) over time. Optimal battery sizing using the Firefly algorithm (FA) was applied, which can reduce the cost of the microgrid and achieve optimal battery sizing [16], [17].

However, combining renewable energy sources with batteries can cause high fluctuations in battery charging and discharging, leading to a shorter battery lifetime and a higher replacement cost. Therefore, this paper proposes a technique for optimizing the capacity and cost of the hybrid ESS combining battery and supercapacitor in a standalone DC microgrid. A low-pass filter is used to separate the low-frequency power needed to charge and discharge the battery and the high-frequency part is allocated to the supercapacitor. Several techniques are currently used for optimization tasks, including Particle Swarm Optimization (PSO) and Firefly Algorithm (FA) and Whale Optimization Algorithm (WOA). Each optimization technique has a different solution, parameters, and performance. The WOA technique is relatively unique since it is able to obtain a quick solution by using a small number of iterations [18], [19]. Moreover, the WOA has the ability to maintain the balance between exploration and exploitation during the search process and has no velocity tracking for each individual in the population, thus reducing computational overhead compared to the PSO-based approach. It is found that there are no studies using the WOA technique for optimal capacity and cost analysis of hybrid ESS in DC microgrids. Therefore, this paper applies the WOA method to the optimization of the capacity and cost of a hybrid ESS combining battery and supercapacitor in a standalone DC microgrid.

The salient features of the paper are summarized as follows:

1) This paper proposes a method for optimal capacity and cost analysis of the hybrid ESS with a battery and a supercapacitor in a standalone DC microgrid. A filter-based approach is employed to separate different frequency components of microgrid active powers and allocate them to the hybrid ESS. The high-frequency component of the active power is supplied by the supercapacitor, while the low frequency component of the active power is provided by the battery. Thus, frequent charge and discharge of the battery is decreased, extending battery lifetime and reducing battery replacement costs.
2) Due to its simplicity of implementation, the Whale optimization algorithm (WOA) is applied to optimize the cut-off frequency of the low-pass filter and obtain the optimal sizing of the hybrid ESS using yearly real data on load demand, wind turbine and PV power generations. Compared to the only-battery case study, the total cost of the hybrid ESS throughout the entire project is reduced by 12.01% compared to the only-battery case.

The rest of this paper is structured as follows. Section II explains the microgrid. Section III introduces hybrid energy storage systems. The theory of the Whale optimization algorithm is given in Section IV. Section V provides the methodology of this work, whereas Section VI verifies the performance of the proposed strategy. Finally, Section VII concludes the paper.

II. DESCRIPTION OF DC MICROGRID

A microgrid is a small LV power system, consisting of small scale DGs and loads. Typically, the DGs in the microgrids are mainly from renewable energy sources such as PV and WT systems. In the microgrid system, there are several load types classified based on user types, such as household sectors, commercial building sectors, industrial plants, and various agencies [20]. As mentioned earlier, the ESS is an important part of the energy management

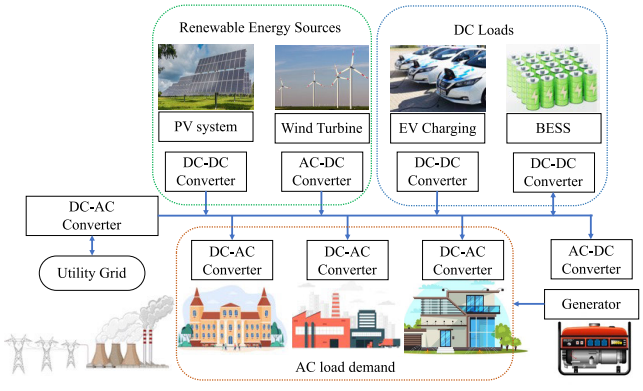

FIGURE 1. Typical components of a DC microgrid system.

system in the microgrid system. The microgrid systems can be classified into DC and AC systems and be operated in two modes: grid-connected and islanded modes. The DC microgrid has been gaining more attention in recent years due to various advantages such as higher conversion efficiency, lower costs of power converters and simpler controllability (as thre is no concern of reactive power, frequency and phase unbalance) [21]. The grid-connected mode of microgrid is stable and able to supply electricity back to the main power grid. In the islanded mode, the microgrid is completely disconnected from the main grid. Therefore, the power used in the standalone microgrid is entirely supplied by the internal power sources. The standalone microgrid is suitable for rural or remote areas. The concept of the standalone microgrid is to generate enough electricity to be used in the control and management systems. The disadvantage of renewable power generation is that it fluctuates and cannot be controlled to meet the load. Therefore, the ESSs are important in the standalone DC microgrid [22], [23]. Figure 1 shows the components of a typical DC microgrid system. DC-DC and DC-AC power converters are crucial parts of the DC microgrid system. The microgrid can be either connected to or disconnected from the main grid. In the DC microgrid system, there are small-scale DG units and local loads. A diesel generator can be used for backup or emergency power generation. The ESS is an essential part of effective energy management within the power system.

III. HYBRID ENERGY STORAGE SYSTEM

Due to the short service life of battery systems, new installations increase costs. This paper explores a hybrid ESS that uses supercapacitors to help extend battery life and uses battery life as an efficiency factor. In this section, the hybrid energy storage system combining a battery and supercapacitor installed in the standalone DC microgrid is briefly explained.

A. BATTERY MODEL

The battery is a high-energy, low-power source and a relatively expensive component of the microgrid system. Thus, battery life is an important economic and reliability factor. The lifespan of the battery needs to be studied and various operating factors that affect its lifespan should be taken into account. The service life of a battery is typically depleted when its current capacity is reduced to 80% of its initial rated capacity. The service life of the battery can be considered in two ways:

- *Battery life cycle:* It is the loss of life caused by the use of the battery. When the battery is operated, it deteriorates depending on the nature of the discharge or charge, the depth of discharge (DoD) and the temperature.
- *Calendar life:* It is the battery's deterioration over time, called aging in calendar years, and it is also affected by temperature. For example, the battery can be used as a backup or emergency power storage device without being used at all. [24].

The mathematical model describing the characteristics of the battery can be defined as,

$$E_b(t+\Delta t) = E_b(t) + [P_{b\_ch}(t)\eta_{b\_ch}]\Delta t, \tag{1}$$

$$E_b(t+\Delta t) = E_b(t) + [P_{b\_dis}(t)\eta_{b\_dis}]\Delta t, \tag{2}$$

$$SoC_b(t) = \frac{E_b(t)}{E_{b\_rated}}, \tag{3}$$

$$SoC_b(t+\Delta t) = SoC_b(t)(1-\beta) + \frac{[P_{b\_ch}\eta_{b\_ch} - P_{b\_dis}\eta_{b\_dis}]}{E_{b\_rated}}\Delta t, \tag{4}$$

where E_b is the capacity of the battery; $P_{b\_ch}(t)$ is the charging power of the battery at time t; $P_{b\_dis}(t)$ is the discharging power of the battery at time t; η_{b_ch} is the charging efficiency of the battery; η_{b_dis} is the discharge efficiency of the battery; E_{b_rated} is the rated capacity of the battery; Δt is the cycle time; $SoC_b(t)$ is the battery state of charge at time t and β is the rate of self-discharge of the battery.

B. SUPERCAPACITOR MODEL

A supercapacitor (SC) is a low-energy and high power source that is typically used in small power grids. The SC is commonly used as a complement to the battery system. High fluctuations in RESs can cause the battery to operate at a high energy rate (depth cycle), shortening its lifespan. The battery may be considered in conjunction with the SC, which can operate at higher power ratings, have more charge and discharge cycles than the battery, and operate at higher temperatures. This increases system reliability and prolongs the service life of the battery in terms of investment.

The SC can operate at high DOD, so it is unnecessary to replace it over its lifetime. The operation of the SC is chemically inert, even at high DoD. Therefore, the high fluctuations in the RESs have no effect on its life. In general, the voltage and temperature of the SC are controllable factors and are constant within the scope of application [25]. Hence, the effect of temperature and voltage on the SC's life can be ignored. In this work, the lifetime of the SC is set to be equal to the calendar year. Similar to the battery, the SC is a bidirectional power source. The mathematical model that described the characteristics of the SC can be defined as,

$$E_{sc}(t+\Delta t) = E_{sc}(t) + [P_{sc\_ch}(t)\eta_{sc\_ch}]\Delta t, \tag{5}$$

$$E_{sc}(t+\Delta t) = E_{sc}(t) + [P_{sc\_dis}(t)\eta_{sc\_dis}]\Delta t, \tag{6}$$

$$SoC_{sc}(t) = \frac{E_{sc}(t)}{E_{sc\_rated}}, \tag{7}$$

$$SoC_{sc}(t+\Delta t) = SoC_{sc}(t)(1-\sigma) + \frac{[P_{sc\_ch}\eta_{sc\_ch} - P_{sc\_dis}\eta_{sc\_dis}]}{E_{sc\_rated}}\Delta t, \tag{8}$$

where E_{sc} is the capacity of the SC; $P_{sc\_ch}(t)$ is the charging power of the SC at time t; $P_{sc\_dis}(t)$ is the discharging power of the SC at time t; η_{sc_ch} is the charging efficiency of the SC; η_{sc_dis} is the discharging efficiency of the SC, E_{sc_rated} is the rated capacity of the SC; $SoC_{sc}(t)$ is the SC state of charge at time t and σ is the rate of self-discharge of the SC.

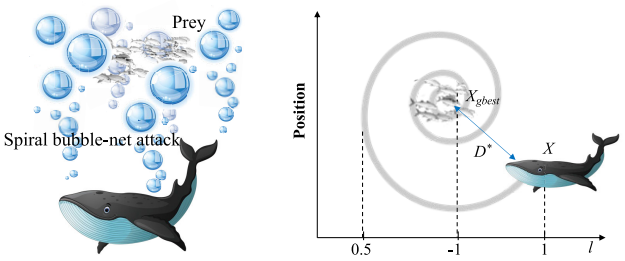

FIGURE 2. Illustration of the WOA-based method.

IV. WHALE OPTIMIZATION ALGORITHM

The whale optimization algorithm (WOA) is a meta-heuristic algorithm [26]. The WOA technique is applied in this study owing to its simplicity and fast approach. The humpback whale's social hunting behavior was applied as an algorithm. Humpback whales are gifted with locomotion in search of food and attack prey with bubble nets. In this way, foraging carried out by humpback whales creates unique bubbles in a circular path. Figure 2 shows Humpback whales breathe underwater and produce bubbles in the form of clouds and pillars. These large groups of bubbles connect to each other and gather bait or schools of fish together. Then, the whales continuously create more bubbles and move to the surface by inhaling and exhaling. The target shrinks by narrowing the bubble circle as it approaches the prey. This hunting of prey appears to aid in finding or capturing the prey by surrounding or immobilizing them. Also, this behavior can hide predators from the prey. The humpback whales can predict the location of their prey so that they can surround it with air bubbles. The whale starts by identifying the best search agent, and then the position of the other search agents is updated using the best search agent. The new search agent location for global search is determined by a randomly selected search agent [27]. Based on the nature of the hunting behavior of humpback whales, the WOA technique employs the hunting behavior that involves encircling prey, bubble-net attacks and random search, as presented in the following sections [28], [29].

A. ENCIRCLING PREY

Humpback whale prey surrounds begin with each whale representing a search. Each individual's position in the search area represents a food source. It is assumed that the current optimal location is the food source or target prey. All search agents in the group will move to the optimal position to surround the prey [30]. Thus, this behavior can be mathematically written as,

$$\overrightarrow{X}(t+1) = \overrightarrow{X}_{gbest}(t) - \overrightarrow{A}\,\overrightarrow{D}, \tag{9}$$

$$\overrightarrow{D} = \left|\overrightarrow{C}\,\overrightarrow{X}_{gbest}(t) - \overrightarrow{X}(t)\right|, \tag{10}$$

where $\overrightarrow{A}$ and $\overrightarrow{C}$ are the coefficient vectors; t is the current iteration; $\overrightarrow{X}_{gbest}(t)$ is the position vector of the best solution obtained at the t-th iteration and $\overrightarrow{X}(t)$ is the current position vector.

The vectors $\overrightarrow{A}$ and $\overrightarrow{C}$ can be calculated as,

$$\overrightarrow{A} = 2\overrightarrow{a}\,r_{rand} - \overrightarrow{a}, \tag{11}$$

$$\overrightarrow{a} = 2 - \frac{2t}{T}, \tag{12}$$

$$\overrightarrow{C} = 2\,r_{rand}, \tag{13}$$

where r_{rand} represents the random vector in [0,1]; $\overrightarrow{a}$ indicates a convergence factor that linearly decreases from 2 to 0 as the number of iterations increases; T is the maximum iteration and t is the current iteration.

B. BUBBLE-NET ATTACKS

For the whale bubble-net attack pattern, it moves upward in a spiral and continuously decreases the circle size, as shown in Figure 2. The humpback whale's prey attack pattern is split into two parts to simulate bubble net behaviors.

- *Shrinking Encircling Mechanism:* This behavior is achieved by reducing the vector from 2 to 0 in (12). The search agent's new location can be set between the current location and the prey's location. This demonstrates the whale's ability to locate local prey.
- *Spiral Updating Position:* Position improvements are made by calculating the sample between each whale's position and the current optimal position of its prey and then simulating the humpback whale's spiral motion to get closer to the best answer. This behavior can be written as,

$$\overrightarrow{X}(t+1) = \overrightarrow{D^*}e^{bl}\cos(2\pi l) + \overrightarrow{X}_{gbest}(t), \tag{14}$$

$$\overrightarrow{D^*} = \left|\overrightarrow{X}(t) - \overrightarrow{X}_{gbest}(t)\right|, \tag{15}$$

where $\overrightarrow{D}^*$ represents the distance between the i-th whale and the current optimal position; b is the constant coefficient used to define the spiral pattern and l is a random number between [0,1].

The whale can swim towards its prey in a spiral shape during hunting while reducing the size of the closed circle. Thus, to model this behavior a probability of 0.5 was set as the criterion to determine how the whale's position should be improved, which can be defined as,

$$\overrightarrow{X}(t+1) = \begin{cases} \overrightarrow{X}_{gbest}(t) - \overrightarrow{A}\,\overrightarrow{D}, & \text{if } p < 0.5, \\ \overrightarrow{D^*}e^{bl}\cos(2\pi l) + \overrightarrow{X}_{gbest}(t), & \text{if } p \geq 0.5. \end{cases} \tag{16}$$

C. RANDOM SEARCH

Random search requires vector $\overrightarrow{A}$ to have a random value greater than 1 or less than -1, and p less than 0.5. The system selects a random search agent to guide the search and increase the searchability of the algorithm. The mathematical model

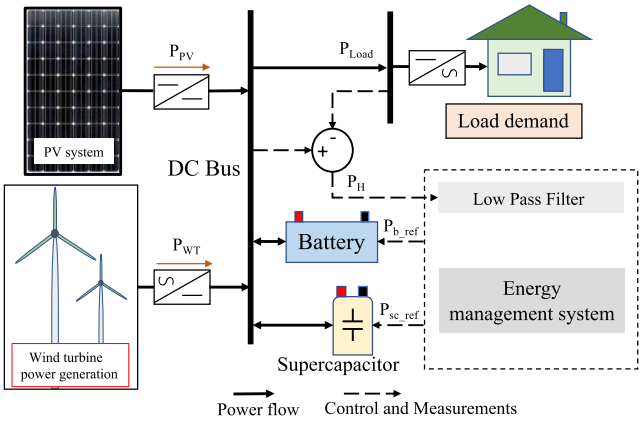

FIGURE 3. Schematic diagram of the standalone DC microgrid with energy management system. In the microgrid system, there are two power sources, namely PV and WT sources, and load demand connected to the common DC bus. A hybrid ESS is responsible for minimizing the active power mismatch between power generation and load demand. A low-pass filter is employed to separate different frequency components of the mismatched active powers.

for this step is determined by,

$$\overrightarrow{D} = \left| \overrightarrow{C}\, \overrightarrow{X}_r(t) - \overrightarrow{X}(t) \right|, \tag{17}$$

$$\overrightarrow{X}(t+1) = \overrightarrow{X}_r(t) - \overrightarrow{A}\, \overrightarrow{D}, \tag{18}$$

where $\overrightarrow{X}_r(t)$ is the random position vector.

V. METHODOLOGY

In this section, the standalone DC microgrid used as a test system in this paper is introduced. Based on the test system, the objective function is proposed and then solved by employing the WOA optimization technique explained in the previous section.

A. STANDALONE DC MICROGRID

A standalone DC microgrid shown in Figure 3 is considered in this paper. In the microgrid system, a residential load, a PV system and a WT system are installed. A hybrid ESS with a battery and SC is also installed to efficiently improve energy management in the system. The main aim of this paper is to optimize the cut-off frequency of the low-pass filter of the hybrid ESS in order to extend battery lifetime under high fluctuations of the RESs and local load demand.

Under standalone DC microgrid operating conditions, the reference active power of the hybrid ESS can be calculated as,

$$P_{H\_ref}(t) = P_{Load}(t) - P_{PV}(t) - P_{WT}(t), \tag{19}$$

where P_{H_ref} is the reference active power of the hybrid ESS; P_{Load} is the active power of the load demand; P_{PV} is the active power of PV generation system and P_{WT} is the active power of WT generation system.

In the case of a hybrid ESS, the reference active power required from the ESS is divided into two parts. The reference active powers are allocated to the battery and the SC using the first-order low-pass filter. It is widely used for active power sharing in hybrid ESS [31], [32]. The smooth or low-frequency component of microgrid active power is fed to the battery, and the high-frequency portion of microgrid active power is supplied by the SC. The power allocation of the hybrid ESS in the s-domain is given by,

$$P_{b\_ref}(s) = P_{H\_ref}(s) \times \frac{1}{1+sT_f}, \tag{20}$$

$$P_{sc\_ref}(s) = P_{H\_ref}(s) - P_{b\_ref}(s), \tag{21}$$

where $T_f = \frac{1}{2\pi f_c}$ and $0 < f_c < \frac{1}{2T_s}$; P_{b_ref} is the reference power of the battery; P_{sc_ref} is the reference power of the supercapacitor; T_f is the time constant of the frequency filter circuit; f_c is the cut-off frequency of the low-pass filter and T_s is the sampling period.

The power allocation depends on the cut-off frequency of the filter (20), which is the parameter to be optimized so that battery lifetime can be extended by decreasing frequent charges and discharges. The cut-off frequency is bounded by the Nyquist principle, i.e., not more than half of the sampling frequency or the Nyquist frequency according to (21).

The reference power of the ESS is used to determine the actual operating power of the hybrid ESS. The operating power of the battery and supercapacitor is obtained by,

$$P_b(t) = \begin{cases} P_{b\_ref}(t)/\eta_{b\_dis}, & P_{b\_ref}(t) > 0, \\ P_{b\_ref}(t)/\eta_{b\_ch}, & P_{b\_ref}(t) < 0, \\ 0, & P_{b\_ref}(t) = 0, \end{cases} \tag{22}$$

$$P_{sc}(t) = \begin{cases} P_{sc\_ref}(t)/\eta_{sc\_dis}, & P_{sc\_ref}(t) > 0, \\ P_{sc\_ref}(t)/\eta_{sc\_ch}, & P_{sc\_ref}(t) < 0, \\ 0, & P_{sc\_ref}(t) = 0, \end{cases} \tag{23}$$

where P_b is the battery's active power and P_{sc} is the supercapacitor's active power. The positive values denote discharging, the negative value charging, and zero the standby state.

The magnitude of the rated power of batteries and supercapacitors can be calculated from the absolute value of the maximum power as,Â

$$P_{b\_rated} = \max(|P_b(t)|), \tag{24}$$

$$P_{sc\_rated} = \max(|P_{sc}(t)|), \tag{25}$$

where P_{b_rated} is the rated power of the battery and P_{sc_rated} is the rated power of the supercapacitor.

The ESS is controlled to operate within the specified DoD for safety and to increase its service life. For this reason, the acceptable DoD is less than 100% and more than 0%. Therefore, when considering the range of DoD, the rated capacity of the battery and supercapacitor are larger than the

baseline capacity and are given as,

$$E_{b\_rated} = \frac{E_{b\_based}}{DoD_{b\_\max} - DoD_{b\_\min}}, \tag{26}$$

$$E_{sc\_rated} = \frac{E_{sc\_based}}{DoD_{sc\_\max} - DoD_{sc\_\min}}, \tag{27}$$

$$E_{b\_based} = \max(E_b(t)) - \min(E_b(t)), \tag{28}$$

$$E_{sc\_based} = \max(E_{sc}(t)) - \min(E_{sc}(t)), \tag{29}$$

where E_{b_based} is the baseline battery capacity; E_{sc_based} is the baseline SC capacity; $DoD_{b\_\max}$ and $DoD_{b\_\min}$ are the upper and lower bounds of the battery depth of discharge; $DoD_{sc\_\max}$ and $DoD_{sc\_\min}$ are the upper and lower bounds of the SC depth of discharge.

B. OBJECTIVE FUNCTION

Objective function is developed in this subsection. The total cost of implementing an ESS in a microgrid system is an important metric for project planning and optimization. This paper uses the total cost of hybrid ESS as an objective function. The cut-off frequency of the low-pass filter is calculated to determine the optimal size of the battery and supercapacitor. The objective function is defined by,

$$\min(NPV_{total}) = C_{install} + NPV_{replace} + NPV_{o\&m}, \tag{30}$$

where NPV_{total} is the net present value of the total cost of the hybrid ESS; $C_{install}$ is the initial installation cost; $NPV_{replace}$ is the net present value of the replacement cost throughout the project and $NPV_{o\&m}$ is the net present value of the operation and maintenance costs throughout the project.

The net present value of the total cost of the hybrid ESS is obtained as the sum of the initial installation cost, the replacement costs and the operation and maintenance costs. Where the initial installation cost of the hybrid ESS is obtained by the sum of the initial installation of the battery and supercapacitor as,

$$C_{install} = C_{b\_install} + C_{sc\_install}, \tag{31}$$

$$C_{b\_install} = (P_{b\_rated} C_{b\_P}) + (E_{b\_rated} C_{b\_E}), \tag{32}$$

$$C_{sc\_install} = (P_{sc\_rated} C_{sc\_P}) + (E_{sc\_rated} C_{sc\_E}), \tag{33}$$

where C_{b_P} is the cost per power of the battery; C_{b_E} is the cost per energy of the battery; C_{sc_P} is the cost per power of the supercapacitor and C_{sc_E} is the cost per energy of the supercapacitor.

As ESS is used, it will deteriorate over time. Replacement costs of battery and supercapacitor can be defined as,

$$NPV_{replace} = NPV_{b\_replace} + NPV_{sc\_replace}, \tag{34}$$

$$NPV_{b\_replace} = \sum_{m=1}^{N_{b\_re}} \frac{C_{b\_install}}{(1+d)^{L_b}}, \tag{35}$$

$$NPV_{sc\_replace} = \sum_{n=1}^{N_{sc\_re}} \frac{C_{sc\_install}}{(1+d)^{L_{sc}}}, \tag{36}$$

where N_{b_re} is the number of battery replacements $(L_P/L_b - 1)$; N_{sc_re} is the number of supercapacitor replacements $(L_P/L_{sc} - 1)$; L_b is the cycle life of the battery; L_{sc} is the cycle life of the supercapacitor and d is the discount rate.

The operation and maintenance costs are obtained from (37), which is the sum of the operation and maintenance costs of the battery and supercapacitor. This paper uses the net present value estimation of the total cost over the life of the project to convert the cost over time to its present value. The uniform series worth factor (USW) equation was applied to convert annual expenses to their present value. The NPVs can be defined as,

$$NPV_{o\&m} = NPV_{b\_o\&m} + NPV_{sc\_o\&m}, \tag{37}$$

$$NPV_{b\_o\&m} = C_{b\_o\&m} E_{b\_rated} \frac{(1+d)^{L_p} - 1}{L_p \cdot (1+d)^{L_p}}, \tag{38}$$

$$NPV_{sc\_o\&m} = C_{sc\_o\&m} E_{sc\_rated} \frac{(1+d)^{L_p} - 1}{L_p \cdot (1+d)^{L_p}}, \tag{39}$$

where $C_{b\_o\&m}$ is the operation and maintenance cost of the battery; $C_{sc\_o\&m}$ is the operation and maintenance cost of the supercapacitor and L_p is the life of the project.

The WOA optimization technique was applied to optimize the cut-off frequency of the low-pass filter. In this paper, we used a total of 100 search agents and a maximum of 30 iterations. The parameters are designed based on the work in [33].

Figure 4 shows the procedure for obtaining the cut-off frequency for the hybrid ESS in the standalone DC microgrid. Determination of the optimum cut-off frequency begins with obtaining the powers of load demand, PV and WT systems. The reference power of the hybrid ESS is then calculated. This reference power is fed to the low-pass filter to obtain the reference powers of the battery and supercapacitor. Also, the rated power and energy of the hybrid ESS are calculated. Then, the battery life and the NPV total cost of the system over the project life are calculated. The iteration is checked, and finally the optimum cut-off frequency is obtained.

VI. SIMULATION RESULTS

The results in this paper are verified using MATLAB running on a MacBook Air (Early 2015), 1.6 GHz Dual-Core Intel Core i5, RAM 8 GB 1600 MHz DDR3. In this study, we used one-year data of load demand, PV and WT systems, as shown in Figures 5, 6 and 7 respectively, for analysis of the entire project life.

Table 1 shows the setup parameters of the hybrid ESS used in this study. The data in the table is taken from [35]. This paper considers a 20-year operation and analyzes the total cost of the hybrid ESS combining a battery and a supercapacitor. A lithium-ion battery was chosen for the analysis due to its widespread use at the present time.

The data of load demand, PV power and WT power generations over 24 hours on 18 June extracted from Figures 5, 6 and 7 are illustrated in Figure 9. The hybrid ESS is responsible for minimizing the active power mismatch between power generation and load demand. Figure 10 shows an example of the active power reference of the hybrid ESS

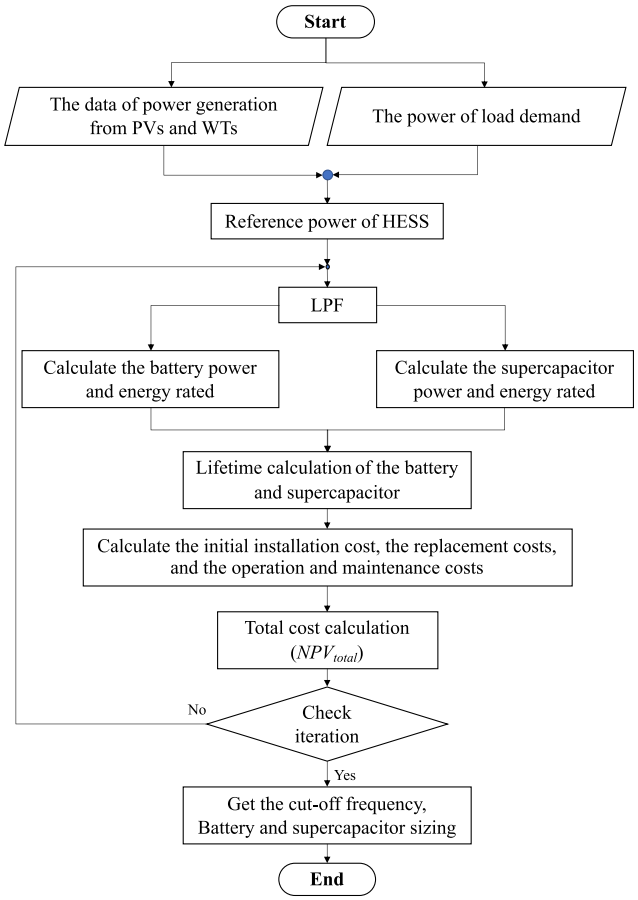

FIGURE 4. Flowchart of the proposed strategy for obtaining an optimal cut-off frequency of the low-pass filter and sizes of the hybrid ESS in the standalone DC microgrid.

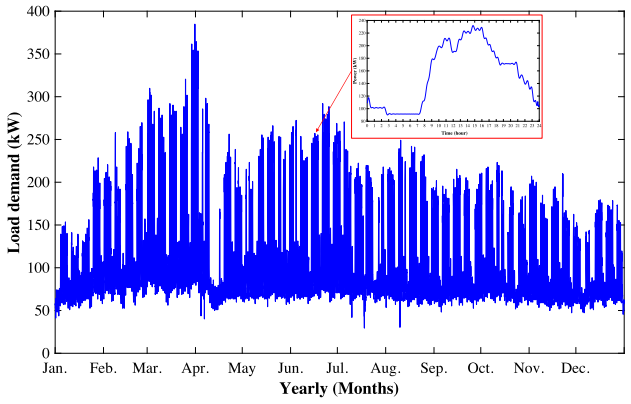

FIGURE 5. One-year of load demand data that was used for verification of the proposed method. The data was provided by Suranaree University of Technology, Thailand.

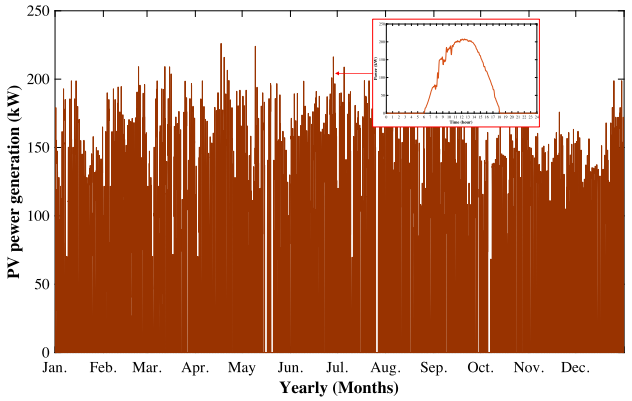

FIGURE 6. One-year active power data of the PV system that was used for verification of the proposed method. The data was provided by Suranaree University of Technology, Thailand.

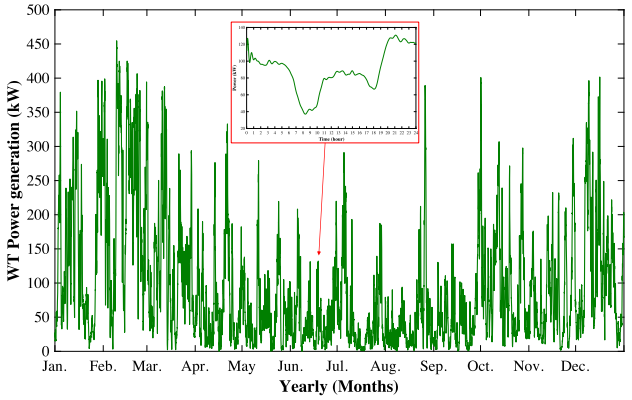

FIGURE 7. One-year active power data of the WT system that was used for verification of the proposed method, taken from [34].

TABLE 1. Setup parameters for verification of the proposed strategy.

Parameter	Value	Unit
C_{b_P}	1200	\$/kW
C_{b_E}	600	\$/kWh
C_{sc_P}	300	\$/kW
C_{sc_E}	2000	\$/kWh
$C_{b\_o\&m}$	19.77	\$/kWh/year
$C_{sc\_o\&m}$	10	\$/kWh/year
L_b	2640	cycles
L_{sc}	5	years
$[SoC_{b\_\min}, SoC_{b\_\max}]$	[20,80]	%
$[SoC_{sc\_\min}, SoC_{sc\_\max}]$	[10,90]	%
$[DoC_{b\_\min}, DoD_{b\_\max}]$	[80,20]	%
$[DoC_{sc\_\min}, DoD_{sc\_\max}]$	[90,10]	%
η_b	90/90	%
η_{sc}	95/95	%
d	5	%
L_P	20	years
σ	1.8	%/day
β	0.13	%/day
T_s	120	seconds

over 24 hours. As it can be seen in the figure, the reference active power of the hybrid ESS contains a high-frequency component. This component can cause frequent charging and discharging of the battery, resulting in a shorter lifetime and a high cost of battery replacement. Thus, hybridization of different technologies of ESSs, such as a battery and a supercapacitor, can prolong battery lifetime and minimize total cost of the entire project.

Figure 8 shows the convergence characteristics of the WOA-based and PSO-based methods. It is clearly seen

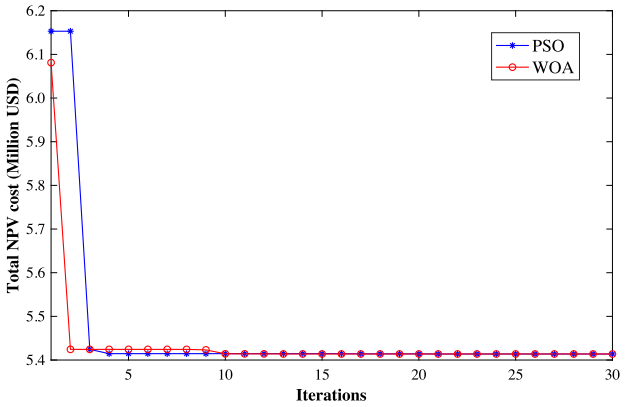

FIGURE 8. Performance convergence curves of the PSO- and WOA-based methods.

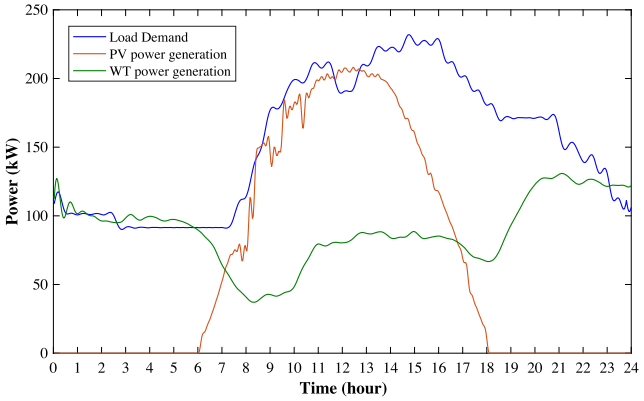

FIGURE 9. Illustration of active powers of load demand, PV power and WT power generations over 24 hours on 18 June extracted from Figures 5, 6 and 7.

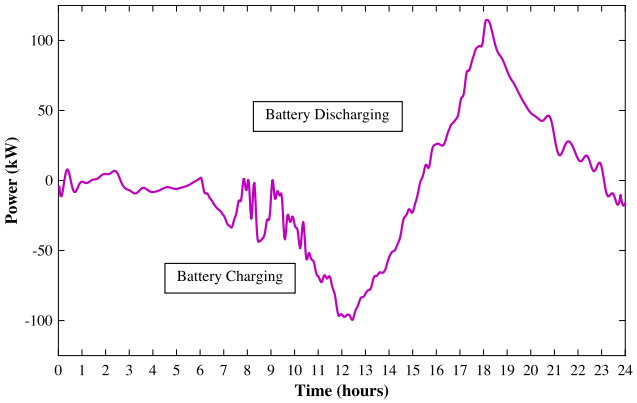

FIGURE 10. Illustration of the active power provided by the hybrid ESS based on PV and WT power generations and load demand in Figure 9, over 24 hours on 18 June.

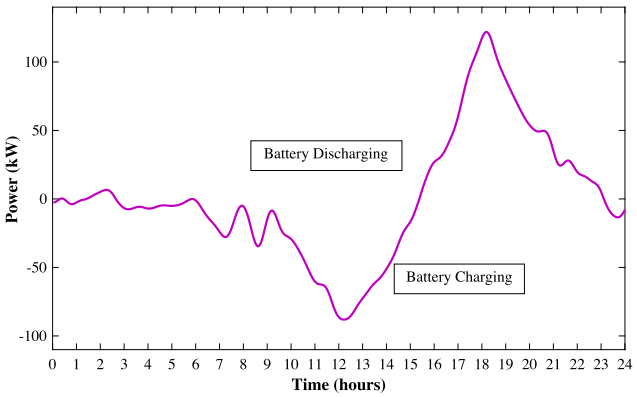

FIGURE 11. Illustration of the active power allocated to the battery over 24 hours on 18 June, with a cut-off frequency of 1.1725mHz.

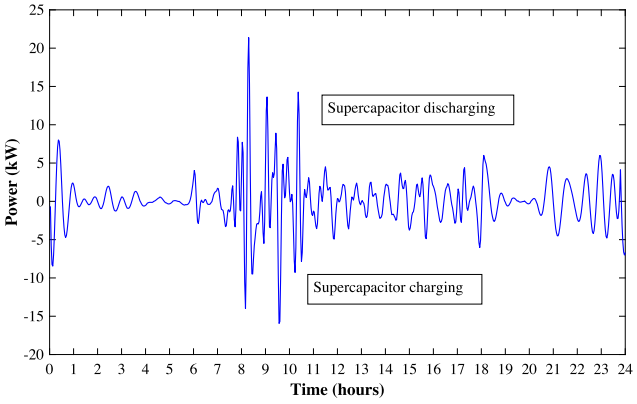

FIGURE 12. An example of active power allocatded to the supercapacitor over 24 hours on 18 June, with a cut-off frequency of 1.1725mHz.

from the convergence characteristic curves that the proposed WOA-based method converges to the optimal value of the total net present value faster than the result obtained by the PSO-based method. The WOA-based method required 15 iterations and 611 seconds to converge to the optimal net present value, whereas the PSO-based method required 21 iterations and 671 seconds.

Table 2 shows the obtained results, including cut-off frequency, rated power and energy of the battery and supercapacitor, respectively. Comparing to using only battery in the microgrid system, the capacity of the battery with hybrid ESS was almost the same at 705.22kWh and 705.23kWh for only battery and hybrid ESS respectively. The simulation results showed that a cut-off frequency of 1.1725mHz is the optimal value for the considered microgrid system. The optimal capacities of the battery and the supercapacitor are 705.23kWh and 3.583kWh respectively.

Figure 11 shows the active power allocation of the battery with a cut-off frequency of 1.1725mHz over 24 hours on 18 June. The battery operated in charging and discharging modes with a smoothed curve. The supercapacitor was responsible for the high-frequency component of the microgrid's active power. Figure 12 depicts active power allocated to the supercapacitor over 24 hours on 18 June. It is evident that the supercapacitor is effective in responding to the high-frequency component of the microgrid's active power.

Table 3 shows the comparison of parameters and costs for only battery and hybrid ESS. The only battery system has a cycle life of 4.68 years with 4 cycles of battery replacement over the project life, whereas the hybrid ESS has a battery life of 4.74 years with 3 cycles of battery replacement

TABLE 2. Optimization results of hybrid ESS.

Parameter	Only Battery	Hybrid ESS	Unit
f_c	-	1.1725	mHz
P_{b_rated}	128.68	129.34	kW
E_{b_rated}	705.22	705.23	kWh
P_{sc_rated}	-	3.583	kW
E_{sc_rated}	-	0.522	kWh

TABLE 3. Comparison of the ESS parameters and costs.

Parameter	Only Battery	Hybrid ESS	Unit
ESS lifetime	4.68	4.74	years
ESS replacements	4	3	times
Initial O&M costs	1,879,659	1,881,970	$
Replacement cost	4,273,399	3,531,876	$
Total NPV cost	6,153,059	5,413,846	$
Total cost reduction	-	12.01*	%

* Compared to only battery case study.

throughout the project life. Due to the high fluctuation of load demand and PV and WT systems, the only battery case study frequently charged and discharged its active power, leading to high battery replacement costs. Therefore, employing a hybrid ESS can reduce the total cost by 12.01% compared to using only battery in the microgrid system.

VII. CONCLUSION

Employing battery storage systems in standalone DC microgrid systems can be cost-inefficient. This paper focused on the optimal capacity and cost analysis of a hybrid ESS, combining a battery and a supercapacitor, in a standalone DC microgrid. The required hybrid ESS' active power was divided into low- and high-frequency components by a low-pass filter. The low frequency of the active power was supplied by the battery, while the high frequency of active power was provided by the supercapacitor. The Whale optimization algorithm was applied to obtain the optimal cut-off frequency of the low-pass filter. The simulation results showed that the battery life increased when the high-frequency component of the active power was provided by the supercapacitor. This is because the number of frequent high-frequency charge/discharge cycles of the battery was reduced, resulting in a smoothed profile. The hybrid ESS reduced the total cost of the entire project by 12.01% compared to the case of employing only the battery. The microgrid system with only the battery has an NPV_{total} of \$6,153,059, whereas the hybrid ESS has an NPV_{total} of \$5,413,846. As a result, the total life-cycle cost of the hybrid ESS is lower than the cost of the battery alone. However, the installed capacity of the supercapacitor had to be increased.

Future work will consider deep neural network-based prediction methods to forecast renewable energy generations and load demands instead of using historical data. Also, a large scale power system will be considered.

REFERENCES

[1] P. Wongdet, T. Boonraksa, P. Boonraksa, W. Pinthurat, B. Marungsri, and B. Hredzak, "Optimal capacity and cost analysis of battery energy storage system in standalone microgrid considering battery lifetime," *Batteries*, vol. 9, no. 2, p. 76, Jan. 2023.

[2] G. G. Farivar, W. Manalastas, H. D. Tafti, S. Ceballos, A. Sanchez-Ruiz, E. C. Lovell, G. Konstantinou, C. D. Townsend, M. Srinivasan, and J. Pou, "Grid-connected energy storage systems: State-of-the-art and emerging technologies," *Proc. IEEE*, vol. 111, no. 4, pp. 397–420, Apr. 2023.

[3] A. A. Kebede, T. Coosemans, M. Messagie, T. Jemal, H. A. Behabtu, J. Van Mierlo, and M. Berecibar, "Techno-economic analysis of lithium-ion and lead-acid batteries in stationary energy storage application," *J. Energy Storage*, vol. 40, Aug. 2021, Art. no. 102748.

[4] J. Carroquino, C. Escriche-Martínez, L. Valiño, and R. Dufo-López, "Comparison of economic performance of lead-acid and Li-ion batteries in standalone photovoltaic energy systems," *Appl. Sci.*, vol. 11, no. 8, p. 3587, Apr. 2021.

[5] R. Zhang, B. Hredzak, and T. Morstyn, "Distributed control with virtual capacitance for the voltage restorations, state of charge balancing, and load allocations of heterogeneous energy storages in a DC datacenter microgrid," *IEEE Trans. Energy Convers.*, vol. 34, no. 3, pp. 1296–1308, Sep. 2019.

[6] T. Morstyn, B. Hredzak, and V. G. Agelidis, "Cooperative multi-agent control of heterogeneous storage devices distributed in a DC microgrid," *IEEE Trans. Power Syst.*, vol. 31, no. 4, pp. 2974–2986, Jul. 2016.

[7] W. Pinthurat and B. Hredzak, "Fully decentralized control strategy for heterogeneous energy storage systems distributed in islanded DC datacentre microgrid," *Energy*, vol. 231, Sep. 2021, Art. no. 120914.

[8] W. Jing, C. Hung Lai, S. H. W. Wong, and M. L. D. Wong, "Battery-supercapacitor hybrid energy storage system in standalone DC microgrids: Areview," *IET Renew. Power Gener.*, vol. 11, no. 4, pp. 461–469, Mar. 2017.

[9] E. Lockhart, X. Li, S. S. Booth, D. R. Olis, J. A. Salasovich, J. Elsworth, and L. Lisell, "Comparative study of techno-economics of lithium-ion and lead-acid batteries in micro-grids in sub-Saharan Africa," Nat. Renew. Energy Lab. (NREL), Golden, CO, USA, Tech. Rep. NREL/TP-7A40-73238, 2019. [Online]. Available: https://www.nrel.gov/docs/fy19osti/73238.pdf?fbclid=IwAR0Abf6vkJZlh64AZnJuPt-hMyfzm9NpWrOgTfNCpzDiavjiMYx_KtWl3vI

[10] F. Li, K. Xie, and J. Yang, "Optimization and analysis of a hybrid energy storage system in a small-scale standalone microgrid for remote area power supply (RAPS)," *Energies*, vol. 8, no. 6, pp. 4802–4826, May 2015.

[11] R. Aazami, O. Heydari, J. Tavoosi, M. Shirkhani, A. Mohammadzadeh, and A. Mosavi, "Optimal control of an energy-storage system in a microgrid for reducing wind-power fluctuations," *Sustainability*, vol. 14, no. 10, p. 6183, May 2022.

[12] C. K. Nayak, K. Kasturi, and M. R. Nayak, "Economical management of microgrid for optimal participation in electricity market," *J. Energy Storage*, vol. 21, pp. 657–664, Feb. 2019.

[13] H. Chen, "Lithium-ion battery-supercapacitor energy management for DC microgrids," *Int. J. Low-Carbon Technol.*, vol. 17, pp. 1452–1458, Feb. 2022.

[14] Y. Jiao and D. Månsson, "Study of the oversized capacity and the increased energy loss of hybrid energy storage systems and design of an improved controller based on the low-pass filter," *J. Energy Storage*, vol. 50, Jun. 2022, Art. no. 104241.

[15] F. Díaz-González, C. Chillón-Antón, M. Llonch-Masachs, S. Galceran-Arellano, J. Rull-Duran, J. Bergas-Jané, and E. Bullich-Massagué, "A hybrid energy storage solution based on supercapacitors and batteries for the grid integration of utility scale photovoltaic plants," *J. Energy Storage*, vol. 51, Jul. 2022, Art. no. 104446.

[16] C. H. B. Apribowo, S. Sarjiya, S. P. Hadi, and F. D. Wijaya, "Optimal planning of battery energy storage systems by considering battery degradation due to ambient temperature: A review, challenges, and new perspective," *Batteries*, vol. 8, no. 12, p. 290, Dec. 2022.

[17] M. Sufyan, N. A. Rahim, C. Tan, M. A. Muhammad, and S. R. S. Raihan, "Optimal sizing and energy scheduling of isolated microgrid considering the battery lifetime degradation," *PLoS ONE*, vol. 14, no. 2, Feb. 2019, Art. no. e0211642.

[18] L. A. Wong and V. K. Ramachandaramurthy, "Optimal allocation of battery energy storage system using WOA-AIS considering net load issue," in *Proc. Int. Conf. Electr., Comput., Commun. Mechatronics Eng. (ICECCME)*, Oct. 2021, pp. 1–6.

[19] P. D. P. Reddy, V. C. V. Reddy, and T. G. Manohar, "Whale optimization algorithm for optimal sizing of renewable resources for loss reduction in distribution systems," *Renewables, Wind, Water, Sol.*, vol. 4, no. 1, pp. 1–13, Dec. 2017.

[20] X. Zhou, T. Guo, and Y. Ma, "An overview on microgrid technology," in *Proc. IEEE Int. Conf. Mechatronics Autom. (ICMA)*, Aug. 2015, pp. 76–81.
[21] F. S. Al-Ismail, "DC microgrid planning, operation, and control: A comprehensive review," *IEEE Access*, vol. 9, pp. 36154–36172, 2021.
[22] R. Kandari, N. Neeraj, and A. Micallef, "Review on recent strategies for integrating energy storage systems in microgrids," *Energies*, vol. 16, no. 1, p. 317, Dec. 2022.
[23] M. Abbasi, E. Abbasi, L. Li, R. P. Aguilera, D. Lu, and F. Wang, "Review on the microgrid concept, structures, components, communication systems, and control methods," *Energies*, vol. 16, no. 1, p. 484, Jan. 2023.
[24] H. Wang, T. Wang, X. Xie, Z. Ling, G. Gao, and X. Dong, "Optimal capacity configuration of a hybrid energy storage system for an isolated microgrid using quantum-behaved particle swarm optimization," *Energies*, vol. 11, no. 2, p. 454, Feb. 2018.
[25] L. Zhang and J. Zhang, "Capacity optimal research of hybrid energy storage systems for stand-alone wind/PV micro-grid," *DEStech Trans. Environ., Energy Earth Sci.*, vol. 1, Nov. 2016.
[26] M. Seyedali and L. Andrew, "The whale optimization algorithm," *Adv. Eng. Softw.*, vol. 95, pp. 51–67, May 2016.
[27] S. Chakraborty, A. K. Saha, S. Sharma, S. Mirjalili, and R. Chakraborty, "A novel enhanced whale optimization algorithm for global optimization," *Comput. Ind. Eng.*, vol. 153, Mar. 2021, Art. no. 107086.
[28] H. Ding, Z. Wu, and L. Zhao, "Whale optimization algorithm based on nonlinear convergence factor and chaotic inertial weight," *Concurrency Comput., Pract. Exper.*, vol. 32, no. 24, p. e5949, Dec. 2020.
[29] P. Sohrabi, H. Dehghani, and R. Rafie, "Forecasting of WTI crude oil using combined ANN-whale optimization algorithm," *Energy Sources, B, Econ., Planning, Policy*, vol. 17, no. 1, Dec. 2022, Art. no. 2083728.
[30] T. Boonraksa, P. Boonraksa, B. Marungsri, and S. L. Leiwynn, "Location and sizing optimization of distributed generation systems on smart grid with the whale optimization algorithm," in *Proc. 9th Int. Electr. Eng. Congr. (iEECON)*, 2021, pp. 81–84.
[31] V. Miñambres-Marcos, M. Guerrero-Martínez, F. Barrero-González, and M. Milanés-Montero, "A grid connected photovoltaic inverter with battery-supercapacitor hybrid energy storage," *Sensors*, vol. 17, no. 8, p. 1856, Aug. 2017.
[32] Q. Xu, X. Hu, P. Wang, J. Xiao, P. Tu, C. Wen, and M. Y. Lee, "A decentralized dynamic power sharing strategy for hybrid energy storage system in autonomous DC microgrid," *IEEE Trans. Ind. Electron.*, vol. 64, no. 7, pp. 5930–5941, Jul. 2017.
[33] M. Tahmasebi, J. Pasupuleti, F. Mohamadian, M. Shakeri, J. M. Guerrero, M. R. Basir Khan, M. S. Nazir, A. Safari, and N. Bazmohammadi, "Optimal operation of stand-alone microgrid considering emission issues and demand response program using whale optimization algorithm," *Sustainability*, vol. 13, no. 14, p. 7710, Jul. 2021.
[34] J. Sandoval. *Wind Power Generation Data*. Accessed: Mar. 3, 2023. [Online]. Available: https://www.kaggle.com/datasets/jorgesandoval/wind-power-generation?resource=download&fbclid=IwAR0_ahT3HoPTbB8To0qeOKcKuDYxtlW1FEGCncrYnapvThG9bxChKY31lYk
[35] *2022 Grid Energy Storage Technology Cost and Performance Assessment*. Accessed: Mar. 3, 2023. [Online]. Available: https://www.energy.gov/eere/analysis/2022-grid-energy-storage-technology-cost-and-performance-assessment

TERAPONG BOONRAKSA was born in Sakon Nakhon, Thailand, in 1989. He received the B.Eng. degree in electrical engineering from Kasetsart University, Chalermphrakiat Sakhon Nakhon Province Campus, in 2012, and the M.Eng. and D.Eng. degrees in electrical engineering from the Suranaree University of Technology, Thailand, in 2014 and 2020, respectively. He is currently an Assistant Professor with the School of Electrical Engineering, Rajamangala University of Technology Rattanakosin, Thailand. His current research interests include electrical power systems, smart grid technology, and electric vehicle technology.

WATCHARAKORN PINTHURAT received the M.E. degree in energy engineering from the Asian Institute of Technology, Bangkok, Thailand, in 2016. He is currently with the Department of Electrical Engineering, Rajamangala University of Technology Tawan-ok, Chanthaburi, Thailand. His current research interests include the control of distributed energy storage systems, the applications of deep reinforcement learning for distributed energy storage systems, and hybrid energy storage systems.

PINIT WONGDET was born in Nakhon Ratchasima, Thailand, in 1995. He received the B.Eng. and M.Eng. degrees in electrical engineering from the Suranaree University of Technology, Nakhon Ratchasima, in 2016 and 2019, respectively. He was with School of Electrical Engineering, Suranree University of Technology, Thailand. After, the search has done and submitted to the journal, he then joined the Provincial Electricity Authority (PEA), Thailand. His current research interests include renewable energy, storage systems, and microgrids.

PROMPHAK BOONRAKSA was born in Sakon Nakhon, Thailand, in 1990. She received the B.Sc. degree in applied physics, the M.Eng. degree in electronics engineering, and the D.Eng. degree in electrical engineering from the King Mongkut's Institute of Technology Ladkrabang, Thailand, in 2012, 2014, and 2020, respectively. Currently, she is with the School of Electrical Engineering, Rajamangala University of Technology Suvarnabhumi, Thailand. Her research interests include photovoltaic systems, semiconductor devices, and renewable energy.

BOONRUANG MARUNGSRI (Member, IEEE) was born in Nakhon Ratchasima, Thailand, in 1973. He received the B.Eng. and M.Eng. degrees in electrical engineering from Chulalongkorn University, Thailand, in 1996 and 1999, respectively, and the D.Eng. degree in electrical engineering from Chubu University, Kasugai, Aichi, Japan, in 2006. He is currently an Assistant Professor with the School of Electrical Engineering, Suranaree University of Technology, Thailand. His current research interests include electrical power and energy systems and high-voltage insulation technologies.

BRANISLAV HREDZAK (Senior Member, IEEE) received the B.Sc. and M.Sc. degrees in electrical engineering from the Technical University of Kosice, Kosice, Slovak, in 1993, and the Ph.D. degree in electrical engineering from the Napier University of Edinburgh, Edinburgh, U.K., in 1997. He was a Lecturer and a Senior Researcher in Singapore from 1997 to 2007. He is currently a Senior Lecturer with the School of Electrical Engineering and Telecommunications, University of New South Wales, Sydney, NSW, Australia. His current research interests include the control of distributed renewable energy sources, hybrid storage technologies, and advanced control systems for power electronic converters and energy storage systems.